Dispersion Effects in an Actively Mode-Locked Inhomogeneously Broadened Laser

Wei Lu, Li Yan, *Member, IEEE*, and Curtis R. Menyuk, *Fellow, IEEE*

***Abstract*—We theoretically and experimentally studied the dispersion effects in an actively mode-locked inhomogeneously broadened laser. In the positive group velocity dispersion (GVD) region, the laser generates incoherent pulses. Self-phase modulation and resonant dispersion impede reduction of the pulse duration when the GVD is small or near zero. A single, stable, soliton-like pulse can be generated only when the GVD is within a certain range of negative values. When the negative GVD is too small, the laser generates only multiple soliton-like pulses because of excess gain filtering. When the negative GVD is too large, the soliton pulse-shaping process fails, and the laser generates only incoherent pulses due to insufficient gain filtering. In the experiment, we characterized an actively mode-locked inhomogeneously broadened Nd : silicate glass laser and confirmed this GVD dependence. The laser generated self-sustaining, soliton-like pulses as short as 77 fs.**

***Index Terms*—Dispersion, inhomogenously broadened lasers, mode-locked lasers, Nd:glass laser, soliton.**

I. Introduction

BROAD-BAND solid-state lasers are of interest for generation of ultrashort pulses. There have been many theoretical and experimental works on modelocking of broad-band solid-state lasers. Most of them focus on homogeneously broadened lasers. Since the gain of a homogeneously broadened laser is analytically easy to describe, theories of modelocking have been well established, and the modelocking dynamics have been well understood. In the absence of self-phase modulation (SPM), actively mode-locked homogeneously broadened lasers can always generate coherent pulses, and the minimum pulsewidth occurs when the group velocity dispersion (GVD) is equal to zero [1], [2]. With the presence of SPM, a stable pulse can be shortened by a factor up to 2.5 around zero GVD until the onset of instability due to excessive SPM [3]. Due to soliton pulse shaping, an even larger pulse shortening can be achieved in the negative GVD region, as long as the GVD is more negative than a minimum amount to maintain stable soliton-like pulses [4]. Generally, the resonant dispersion from the gain medium has a negligible effect on the modelocking process for a homogeneously broadened laser [5]. On the other hand, generation of coherent pulses from inhomogeneously broadened lasers is often not guaranteed. Studies have shown that positive GVD impedes generation of coherent pulses in a purely actively mode-locked inhomogeneously broadened laser when the lasing bandwidth is too large [6], [7]. Experiments also show that an actively mode-locked laser cannot generate coherent pulses even at zero GVD and can only generate soliton-like pulses under certain conditions [8]. The roles played by the nonlinearity, GVD, and resonant dispersion in active modelocking of an inhomogeneously broadened laser have not been studied and understood.

In this paper, we present results of a comprehensive numerical and experimental study of the dispersive effects in an actively mode-locked inhomogeneously broadened laser. We take into account the nonresonant GVD, resonant dispersion from the gain medium, and SPM in the numerical simulation. Modelocking performance in all GVD regions is simulated, which shows some unique behaviors for an inhomogeneously broadened laser. Experimentally, we have characterized an actively mode-locked inhomogeneously broadened Nd : silicate glass laser in different GVD regions, and the results agree with the numerical simulation. In Section II, we describe the model and numerical study. In Section III, we present the experimental results. We give the conclusions in Section IV.

II. Theoretical Study

A. The Model

In modeling the active modelocking process, we include the actions of the gain, dispersion, active-amplitude (AM) modulation, SPM, and self-amplitude modulation (SAM). In the case of a homogeneously broadened laser, the modelocking dynamics can be described by a master equation in the time domain and closed-form solutions can be found in most cases [3], [4]. By contrast, in the case of an inhomogeneously broadened laser, the complexity of the inhomogeneous gain saturation makes it difficult to describe the modelocking dynamics in the time domain. Hence, we treat the gain, dispersion, and sinusoidal AM modulation in the frequency domain, and the SPM and SAM in the time domain. The evolution of complex electric fields $\tilde{E}_n$ and $\tilde{E}(t)$ in the frequency and time domains, respectively, are governed by the following coupled ordinary differential equations

$$T_R\frac{d\tilde{E}_n}{dT} = -\frac{\delta_c}{2}\tilde{E}_n + \frac{\gamma(v_n)p_{m,a}}{2}\tilde{E}_n - j\delta\phi_n\tilde{E}_n + \frac{\Delta_m}{2}(\tilde{E}_{n+1} - 2\tilde{E}_n + \tilde{E}_{n-1}) \quad (1)$$

$$\Delta\tilde{E}(T,t) = (\kappa_{\mathrm{SAM}} - j\kappa_{\mathrm{SPM}})|\tilde{E}(T,t)|^2\tilde{E}(T,t). \quad (2)$$

The time t is the retarded time and T is the round-trip evolution time. The parameters δ_c and T_R are the round trip power loss and

Manuscript received December 12, 2001; revised May 7, 2002. This work was supported by the National Science Foundation under Grant 9703988.

W. Lu and L. Yan are with the Department of Computer Science and Electrical Engineering, University of Maryland, Baltimore County, Baltimore, MD 21250 USA.

C. R. Menyuk is with the Department of Computer Science and Electrical Engineering, University of Maryland, Baltimore County, Baltimore, MD 21250 USA and also with PhotonEx Corporation, Maynard, MA 01754 USA.

Publisher Item Identifier 10.1109/JQE.2002.802985.

transit time, respectively, while Δ_m is the modulation index of the AM modulation function

$$t_{\mathrm{AM}}(t) = 1 - \Delta_m(1 - \cos\omega_m t). \tag{3}$$

The inhomogeneously broadened gain $\gamma(v_n)$ is given by

$$\gamma(v_n) = \sum_{v_\xi} \gamma(v_\xi, v_n) \tag{4}$$

where $\gamma(v_\xi, v_n)$ is the gain contributed from the homogeneous group of atoms ξ. Under the fast gain approximation, $\gamma(v_\xi, v_n)$ can be expressed as [9]

$$\gamma(v_\xi, v_n) = \frac{\gamma(v_0)}{\eta_0} \frac{p(v_\xi) dv_\xi \overline{g}(v_n - v_\xi)}{1 + \sum_{v_n} \frac{I(v_n)}{I_s} \overline{g}(v_n - v_\xi)} \tag{5}$$

where $\eta_0 = \int dv_\xi p(v_\xi)\overline{g}(v_0 - v_\xi)$, $I(v_n) = |E(v_n)|^2$ is the intensity of the nth mode, and I_s is the homogeneous saturation intensity. For a general inhomogeneously broadened laser, for simplicity, we approximate I_s to be the same for all homogeneous groups of atoms. The inhomogeneous broadening is described by the Gaussian distribution $p(v_\xi)$ with a linewidth Δv_{ih}, and $\overline{g}(v_n - v_\xi)$ is the dimensionless Lorentzian lineshape function that has a peak value of unity and a homogeneous linewidth Δv_h. The quantity ϕ_n is the round trip phase shift of the nth mode caused by dispersion and can be written as

$$\phi_n = \frac{1}{2} k'' p_m (\omega_n - \omega_0)^2 - \sum_{v_\xi} \frac{1}{2} \gamma(v_n, v_\xi) p_{\mathrm{m,a}} \frac{2(v_n - v_\xi)}{\Delta v_h}. \tag{6}$$

Here, the first term is the contribution from the GVD, and the second term is from the resonant dispersion due to the gain medium. The resonant dispersion can be expanded in a Taylor series around ω_0 and contains only odd order terms. The linear term gives rise to a net group delay of the whole pulse and can always be compensated by adjusting the cavity length. Thus, in the simulation, we subtracted the linear term from the resonant dispersion. Fig. 1 compares the round-trip phase shift due to the resonant dispersion from the saturated gain with the linear term subtracted to the phase shift due to the GVD. When the GVD is small, the round-trip phase shifts of GVD and resonant dispersion are comparable within the lasing bandwidth. When the GVD is very large, the effect of the resonant dispersion is overwhelmed by the GVD.

We use typical solid-state laser parameters in the simulation. We choose $\Delta v_h = 12\ \mathrm{cm}^{-1}$ and $\Delta v_{\mathrm{ih}} = 48\ \mathrm{cm}^{-1}$. The nonlinear coefficients are $\kappa_{\mathrm{SPM}} = 1.88 \times 10^{-5}\ \mathrm{cm}^2/\mathrm{MW}$ and $\kappa_{\mathrm{SAM}} = \varepsilon\kappa_{\mathrm{SPM}}$, where ε is adjustable. The gain medium is pumped to six times above the threshold, producing an intracavity average intensity of $I_{\mathrm{ave}}/I_s \approx 14.6$. With $I_s = 6.17 \times 10^3\ \mathrm{W/cm}^2$ and assuming an intracavity beam area of $1.2\times10^{-5}\ \mathrm{cm}^2$, the intracavity average power is about 1 W. The active modelocking strength is determined by $\Delta_m f_m^2$, the curvature of the temporal modulation function. A typical modulation frequency is 100 MHz, and the modulation index is about 0.2. To reduce the computation time, we use a model of a short cavity with an axial mode spacing of 2 GHz. We scale down the modulation index to 0.0005 so that the temporal modulation curvature of this modulator in the short cavity is the same as that of a modulator in the long cavity with $f_m = 100$ MHz and $\Delta_m = 0.2$. The short cavity laser produces the same average power as the long cavity laser does. However, the intracavity energy is reduced by 20 times. To account for the same nonlinearity strength, we increase the intracavity intensity by 20 times in (2). We verified that with this proper scaling, the short cavity model ($f_m = 2$ GHz) and the long cavity model ($f_m = 100$ MHz) produce almost the same modelocking behaviors. One example is at $k''p_m = -1000\ \mathrm{fs}^2$ for which a single soliton pulse is formed, and nonlinearity is strong and important.

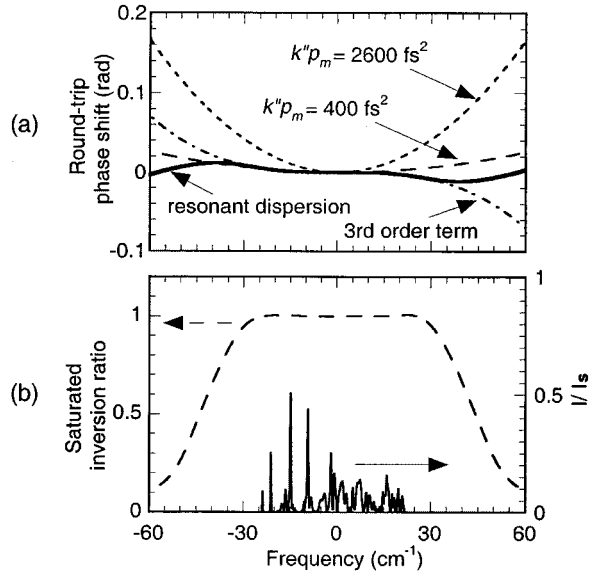

Fig. 1. (a) Round-trip phase shifts due to different kinds of dispersion in an actively mode-locked inhomogeneously broadened laser. (b) Corresponding steady-state saturated inversion ratio and pulse spectrum.

B. Simulation Results

We simulate the modelocking process starting from the free-running state, in which axial modes have random phases. The resulting pulse shape and spectrum are found after 10^5 round trips. Fig. 2(a) shows the pulsewidth dependence on the GVD without SAM by setting $\varepsilon = 0$ ($\kappa_{\mathrm{SAM}} = \varepsilon\kappa_{\mathrm{SPM}}$). The simulated pulse bandwidths are nearly the same around 40 cm^{-1}, as dominantly governed by the inhomogeneous linewidth. We discuss in detail the modelocking behavior in different GVD regions. For comparison, Fig. 2(b) shows the pulsewidth dependence on the GVD for a purely homogeneously broadened laser with the same gain linewidth and intracavity pulse energy, which is discussed at the end of this section.

1) Positive GVD Region: Earlier, Yan studied the pulse coherence of an actively mode-locked inhomogeneously broadened laser in the absence of SPM and resonant dispersion [6]. In an extremely inhomogeneously broadened laser, spectral narrowing by the gain is negligible, and the modulator attempts to overcome the impairment of GVD. In this case, a GVD-limited maximum-lockable optical bandwidth $\Delta v_{\mathrm{p,lock}}$ is given by [6]

$$\Delta v_{\mathrm{p,lock}} = \left[\frac{2^{3/2}\ln 2}{\pi}\right]^{1/2} \left[\frac{\Delta_m f_m^2}{k''p_m}\right]^{1/4}. \tag{7}$$

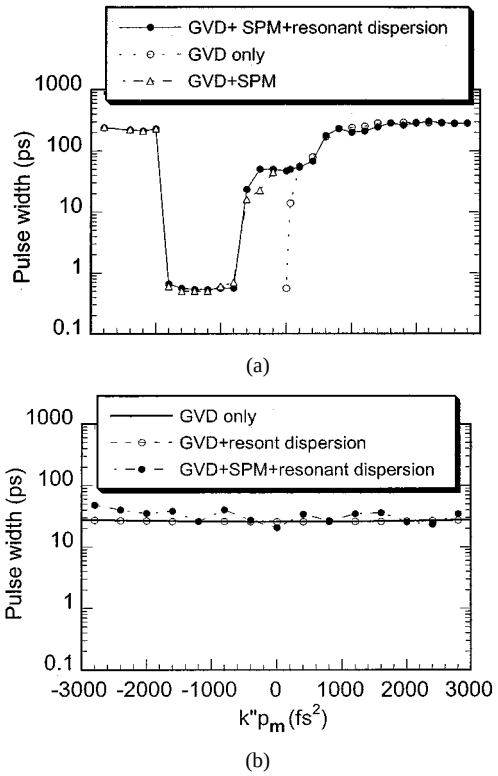

Fig. 2. Simulated pulsewidths in different GVD regions in: (a) an inhomogeneously broadened laser and (b) a purely homogeneously broadened laser.

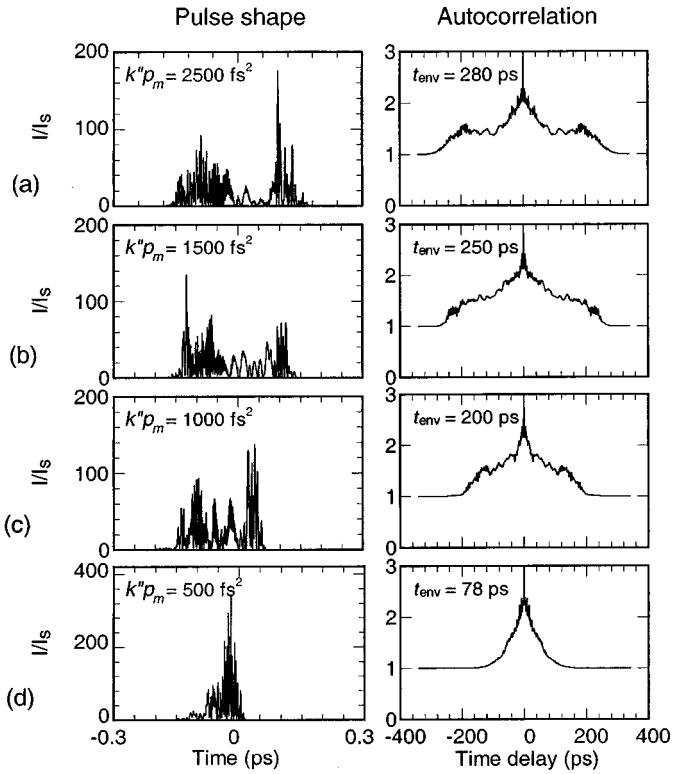

Fig. 3. Simulated pulse shapes and autocorrelation traces in the positive GVD region. (a) $k''p_m = +2500$ fs^2. (b) $k''p_m = +1500$ fs^2. (c) $k''p_m = +1000$ fs^2. (d) $k''p_m = +500$ fs^2

When the laser's lasing bandwidth is within this lockable bandwidth, active modelocking can generate coherent pulses. When the lasing bandwidth is larger than this lockable bandwidth, the laser pulses are partially coherent.

Fig. 3 shows the pulse shape and corresponding autocorrelation trace with different amounts of positive GVD. Clearly, the pulses are incoherent, with multiple spikes distributed over a broad time interval. As shown in Fig. 2(a), when the GVD is larger than $+200$ fs^2, GVD impedes the generation of a coherent pulse. This result is consistent with (7), since at $k''p_m = +200$ fs^2, the lockable bandwidth $\Delta v_{\mathrm{p,\,lock}} = 1.8$ cm^{-1}, which is already much smaller than the lasing bandwidth. The resonant dispersion causes a drift of the pulse from the transmission peak of the modulation function, as shown in Fig. 3, and the drift becomes more obvious when the GVD is smaller. We also notice that when the GVD is very large ($>+2000$ fs^2), the pulsewidth does not increase much.

2) Near-Zero GVD: From (7), we find that the maximum lockable bandwidth increases as the GVD decreases, and with a sufficiently small GVD, the pulse becomes coherent. However, the SPM or resonant dispersion impedes the modelocking when the GVD is reduced nearly to zero. Fig. 4 shows the pulse shape at zero GVD when different effects are considered. Without considering the SPM and resonant dispersion, a coherent pulse of 590 fs is generated, as shown in Fig. 4(a). When the SPM or resonant dispersion is included, the laser can generate only incoherent pulses of tens of picoseconds, as shown in Fig. 4(b) and (c), respectively. Apparently, the SPM broadens the pulse spectrum. As the broadened spectrum is comparable to the gain linewidth, due to the gain-filtering effect, the pulse becomes distorted and breaks into an incoherent pulse. When only the res-

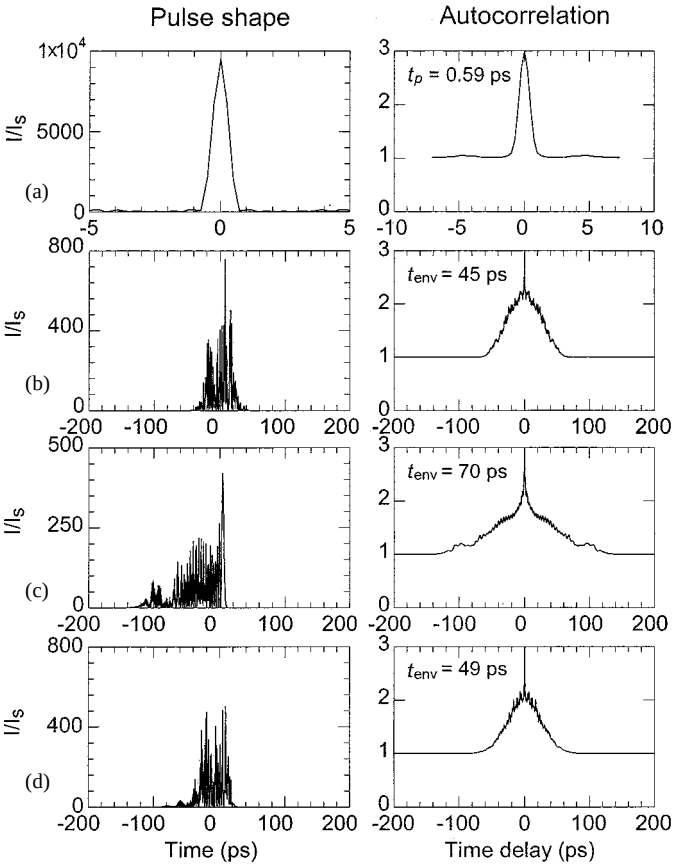

Fig. 4. Simulated pulse shapes and autocorrelation traces at zero GVD due to different effects. (a) Without resonant dispersion and SPM. (b) With additional SPM. (c) With additional resonant dispersion. (d) With resonant dispersion and SPM.

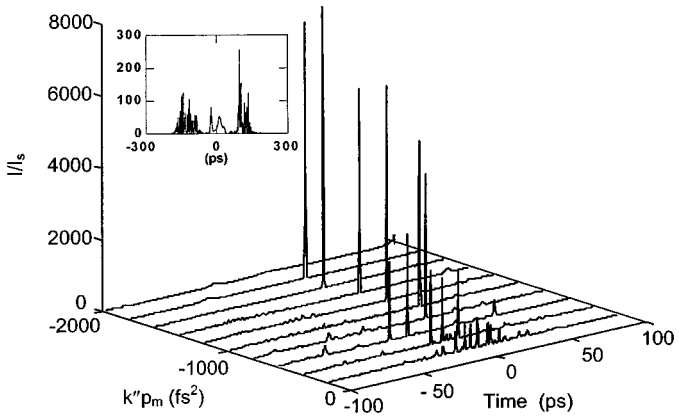

Fig. 5. Simulated pulse shapes with different amounts of negative GVD and without the resonant dispersion. The inset is the full pulse shape when $k''p_m = -2000$ fs^2.

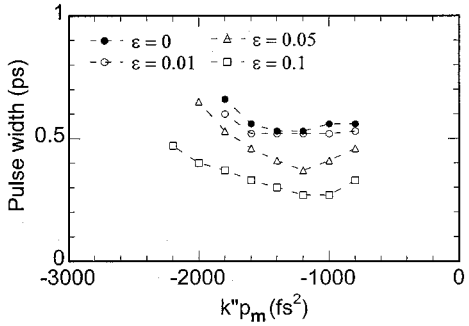

Fig. 6. Simulated regime for generation of single soliton-like pulse with different strength of SAM.

onant dispersion is present, the pulse shape is asymmetric with an oscillatory structure at the leading edge, a typical characteristic due to an odd-order dispersion [10]. Within the lasing spectrum ($\pm\sim$25 cm^{-1}), the resonant dispersion is mainly from the third-order term. Simulation shows that this third-order term, with $\phi'''_{\rm res} \approx -6.88 \times 10^5$ fs^3 that is nearly one order of magnitude larger than the nonresonant third-order dispersion from intracavity components for typical solid-state lasers, produces a pulse shape similar to that in Fig. 4(c). Because of the negative resonant third-order dispersion, both the long- and short-wavelength components travel ahead of the central portion of the pulse spectrum and interfere to produce sharp spikes. We notice that when both the resonant dispersion and SPM are present, the pulsewidth is narrower than that with the resonant dispersion alone, as shown in Fig. 4(d). A plausible explanation is that, for the spikes that are already near the extremities of spectrum, spectral broadening by the SPM moves energies outside the gain linewidth. As a result, these spikes experience more loss and are attenuated, forcing redistribution of spectral components in the time domain.

3) Negative GVD Region: In the negative GVD region, the soliton pulse shaping can provide a mechanism to generate coherent and short pulses. However, as shown in Fig. 2, the laser still generates incoherent pulses when the negative GVD is small. To examine the role of the GVD, we simulate the modelocking performance without the resonant dispersion, as shown in Fig. 5. Between zero GVD and -300 fs^2, only multispike incoherent pulses are produced. Between -300 fs^2 and -750 fs^2, distinct triple or double pulses are formed, with some unsuppressed low intensity noise spikes. When the GVD is more negative, cleaner, single soliton-like pulses are generated. However, when the GVD is beyond -2100 fs^2, the laser again generates only incoherent pulses with envelope duration longer than 200 ps, similar to what happens in the positive GVD region. These mode-locking behaviors can be explained as follows. The soliton pulse is the result of interplay between the negative GVD and SPM, and the pulsewidth is given by [11]

$$t_p = 3.53\frac{|k''p_m|}{\kappa_{\rm spm} W_p} \tag{8}$$

where W_p is the intracavity pulse energy fluence. Given the same intracavity pulse energy, the pulsewidth decreases as the negative GVD decreases. The minimum pulsewidth, however, is limited by the gain linewidth. The AM modulation initially produces many uncorrelated spikes with duration approximately equal to the inverse of the lasing bandwidth. In the small negative GVD region, many spikes already satisfy the relationship (8), and these uncorrelated spikes, together with a low-intensity continuum, form an incoherent pulse. As the negative GVD increases, more energy is needed for a soliton, and the number of soliton-like spikes decreases. Since the GVD is not large enough yet to disperse the continuum noises efficiently, they are not completely suppressed by the amplitude modulation [3], [4]. When the negative GVD increases further, a single soliton-like pulse is generated. With very large negative GVD, the soliton-like pulse broadens, and its bandwidth decreases. When the bandwidth of the soliton-like pulse is narrower than the free-running lasing bandwidth, the nonsoliton spectral components, which are supported by the gain, distort the pulse and eventually destabilize the soliton-like pulse shaping process. In this regime, only the AM modulation contributes to the pulse shaping, and one obtains an incoherent pulse similar to that in the positive GVD region. This generation of incoherent pulse due to the gain under-filtering effect has no counterpart in a homogeneously broadened laser and only exist in a broad-band inhomogeneously broadened laser. The resonant dispersion further impairs the pulse, which increases the necessary negative GVD for a transition from an incoherent pulse to triple or double soliton-like pulses, but does not change the GVD requirement for generation of a single soliton-like pulse. We notice that the shortest pulse duration does not occur at the smaller boundary of the single soliton pulse regime. This is because near this boundary the mode-locked pulse deviates from an ideal soliton pulse due to the third-order resonant dispersion and the interference from some residual continuum.

In the above study, no SAM is involved. Fig. 6 shows the region for generation of single soliton-like pulse with different strength of SAM. Simulation shows that even with an SAM as strong as $\varepsilon = 0.1$, the modelocking process cannot take place when the AM modulation is turned off at the beginning. Clearly, at this level, the SAM is not sufficient to start the soliton pulse shaping, and modelocking is initiated by the AM modulation. We notice that for different SAM strength, the smaller GVD boundary for generation of single soliton-like pulse re-

mains about the same, which is consistent with the fact that this boundary is due to the limitation of gain linewidth. A stronger SAM, however, removes more effectively the nonsoliton free-running components and thus extends the larger GVD boundary, and the laser generates a shorter pulse, as shown in Fig. 6. In this GVD region, after a single soliton-like pulse is already formed and then setting $\Delta_m = 0$, an SAM as weak as $\varepsilon = 0.01$ can sustain the pulse in the later round trips.

4) Comparison to the Homogeneously Broadened Laser: For a homogeneously broadened laser, strong gain filtering limits the pulse bandwidth that is ~70 times narrower than the inhomogeneously broadened laser in the absence of SPM. With this narrow bandwidth, the GVD effect is negligible, and the pulsewidth remains about 25 ps within the GVD range of ± 3000 fs^2. Furthermore, the resonant dispersion has no impact on the modelocking process, as shown in Fig. 2(b). For the gain linewidth and intracavity pulse energy considered, in the positive GVD region, SPM is substantially larger than the maximum value allowed to maintain stable modelocking [3], resulting in partially coherent pulses that experience complicated variation of pulse shape over different round trips. Our simulation shows that when the GVD is larger than 7000 fs^2, the pulse becomes stable and coherent, while for the inhomogeneously broadened laser, the pulse is always incoherent with a large positive GVD. In the negative GVD region, due to strong gain linewidth limitation, the continuum destabilizes the soliton pulse formation [4] until the GVD is more negative than $-28\,000$ fs^2, beyond which a stable soliton-like pulse can be formed. In contrast, for an inhomogeneously broadened laser, there exists another stability boundary, as discussed earlier.

III. Experimental Study

We experimentally studied the actively mode-locked Nd : silicate glass laser in different GVD regions. Nd : silicate glass has an inhomogeneous linewidth of about 80 cm^{-1} [12]. Its fluorescence linewidth is about 300 cm^{-1}, due to the convolution of the inhomogeneous broadening and multiple Stark-split transitions. The one-phonon and two-phonon processes rapidly thermalize the population distributions among the upper energy levels and lower energy levels [13]. As a result, in the free-running state or when the modelocking force is relatively weak, only one or two Stark-split transitions are involved, and the Nd : glass behaves "less inhomogeneously broadened" [6]. When one uses a single transition line to model the multiple Stark-split transitions, the effective inhomogeneous linewidth for Nd : silicate glass is about 44 cm^{-1} [14], close to the parameters used in the numerical simulation.

A schematic diagram of the experimental setup is shown in Fig. 7. The cavity was formed by two concave mirrors with radii of curvature equal to 10 cm, a high-reflection mirror, and an output coupler with transmittance of ~2%. A Nd : silicate glass (LG-680) plate with thickness of 4.5 mm was placed at the Brewster's angle and used as the gain medium. The two concave mirrors were tilted at an incident angle of ~9°. An acoustooptic modulator (AOM) was placed at the end of one arm. The solid line represents the dispersion-uncompensated cavity. To adjust the GVD, a pair of SF-10 prisms was added in the other arm

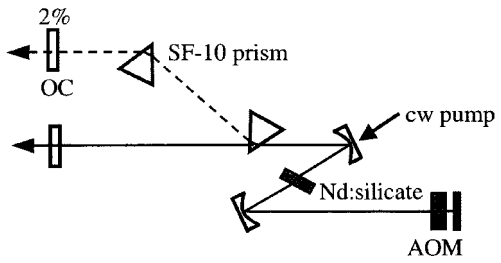

Fig. 7. Schematic diagram of the actively mode-locked Nd : silicate glass laser.

as shown by the dashed line. By adjusting the separation of the prisms, we were able to compensate the positive GVD and move the net GVD into the negative region. A cw Ti : sapphire laser was tuned at ~810 nm to pump the Nd : glass. The AOM was driven at about 46 MHz, half of the round-trip frequency of the cavity.

For the conventional, dispersion-uncompensated cavity, we estimated the total round-trip GVD to be about $+2600$ fs^2, which includes the contribution from the AOM. In the free-running state (AOM off), the threshold pump power was about 75 mW. At a pump power of ~700 mW, the laser output power was about 34 mW. The continuous-wave (cw) lasing spectrum consists of many spikes and spreads over ~5 nm, with the center wavelength at about 1064 nm, which shows the strong inhomogeneous broadening characteristic of the Nd : silicate glass. To focus on the dispersion effect, we did not purposely flatten the gain profile, and the lasing bandwidth remained nearly the same.

A. Positive GVD Region

When the AOM was turned on, the AM modulation acted to lock the phases of the existing axial modes and did not broaden the bandwidth, as expected for an inhomogeneously broadened laser. Fig. 8 shows the measured pulsewidth dependence on the positive GVD.

When the GVD is larger than $+500$ fs^2, we measured the pulsewidth using a sampling oscilloscope with a response time of ~70 ps. The pulse envelop duration was broadened from 80 to 150 ps when the GVD was increased from $+500$ to $+2000$ fs^2. The time-bandwidth product increased from 100 to 195. With such large time-bandwidth products, the pulses are very incoherent. The pulse duration did not change much when we further increased the GVD. These modelocking characteristics agree with the simulation results in Section II.

When the GVD was reduced to less than $+500$ fs^2, we measured the pulsewidth using an intensity autocorrelator. Fig. 9 shows the autocorrelation traces when the GVD was partially compensated to about $+200$ fs^2 and near zero, respectively. Both autocorrelation traces exhibit a narrow spike superposing on a broad pedestal, which is a characteristic for incoherent pulses. The pulse envelop duration was about 93 and 86 ps, and the time-bandwidth product was about 120 and 110, respectively. In this region, the SPM and resonant dispersion hampers the active modelocking process and prevents the generation of coherent and short pulse, as explained in Section II.

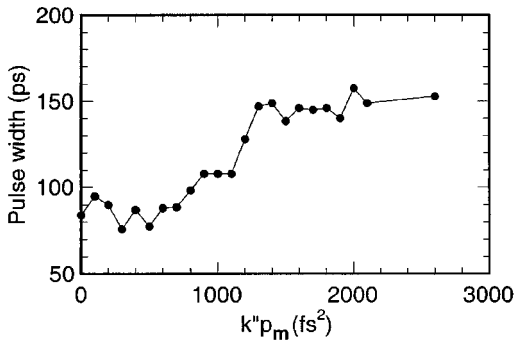

Fig. 8. Measured pulsewidth dependence in the positive GVD region.

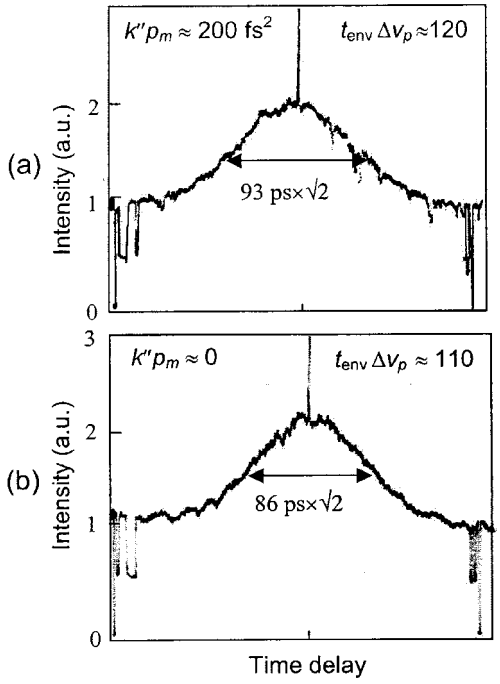

Fig. 9. Measured autocorrelation traces with (a) $k''p_m = +200$ fs^2 and (b) near-zero GVD.

B. Negative GVD Region

The modelocking performance in the negative GVD region is summarized in Fig. 10. When the negative GVD was less than -400 fs^2, we still obtained incoherent pulses with durations of tens of picoseconds. The pulse autocorrelation trace was similar to that in Fig. 9, and the time-bandwidth product was between 85–100. Compared to the small positive GVD region, the pulse coherence does not improve. As explained in Section II, this generation of incoherent pulses is due to the formation of many soliton-like pulses with low peak intensities.

When we increased the negative GVD to about -460 fs^2, the pulsewidth reduced dramatically, and the 3 : 1 ratio of the autocorrelation trace shows that the pulse coherence improves greatly. With increasing negative GVD, the pulse became shorter. At $k''p_m \approx -700$ fs^2, the pulsewidth was about 1.1 ps, with the pulse bandwidth ~4.3 nm, as shown in Fig. 11. In this GVD regime, which we call the transition regime, modelocking was sensitive to cavity alignment or external disturbance. When the negative GVD was larger than -750 fs^2, the pulse was

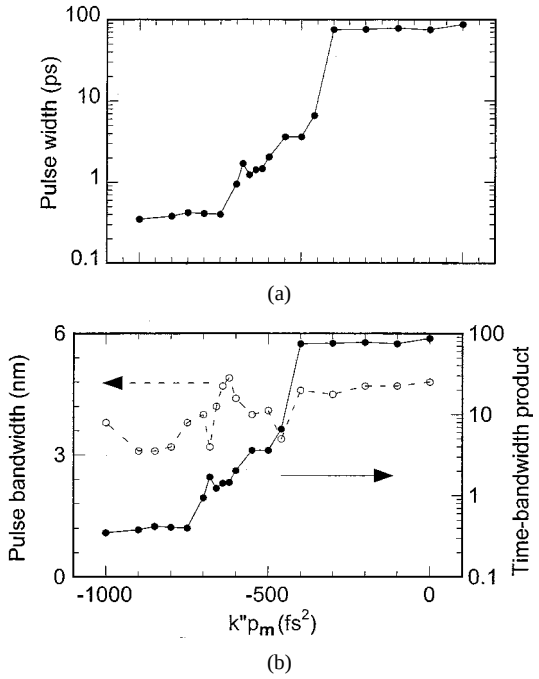

Fig. 10. Measured modelocking performance in the negative GVD region. (a) Pulsewidth dependence on negative GVD. (b) Pulse bandwidth and time-bandwidth product with different negative GVD.

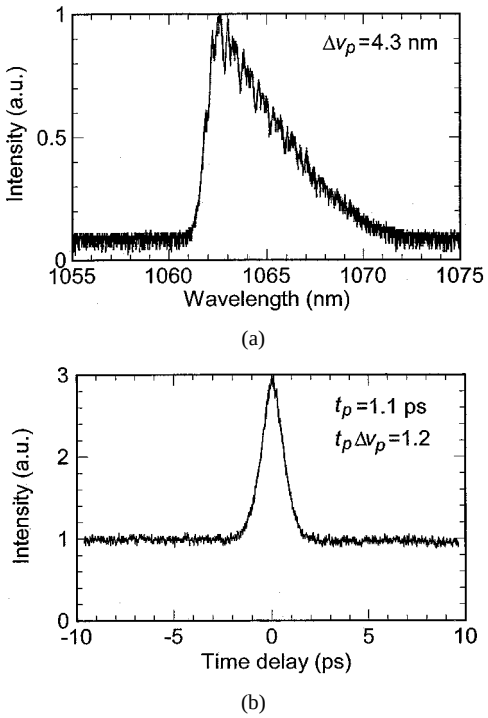

Fig. 11. (a) Pulse spectrum and (b) autocorrelation trace at $k''p_m = -700$ fs^2.

further shortened and became transform limited. Fig. 12(a) shows the pulse autocorrelation trace at $k''p_m \approx -900$ fs^2. The pulsewidth was 350 fs, and the time-bandwidth product was 0.39. At this GVD value, we observed that when we then turned the AOM off, the femtosecond soliton-like pulse could still sustain itself. As shown in Fig. 12(b), the pulsewidth remained at about 320 fs. We notice that the autocorrelation trace of the self-sustaining pulses is smooth while the pulse

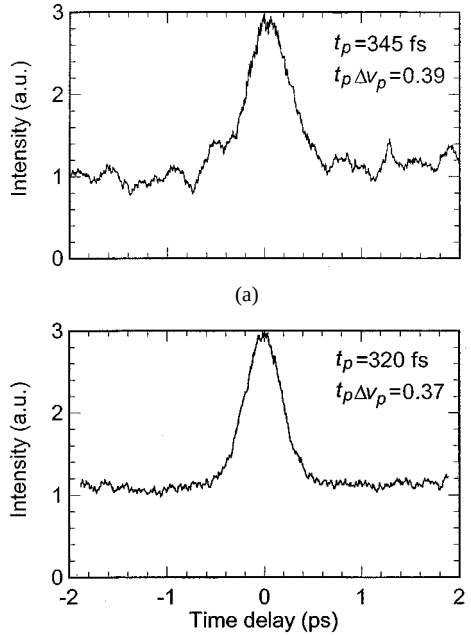

Fig. 12. Measured autocorrelation traces when the AOM is (a) on and (b) off, with $k''p_m = -900$ fs^2.

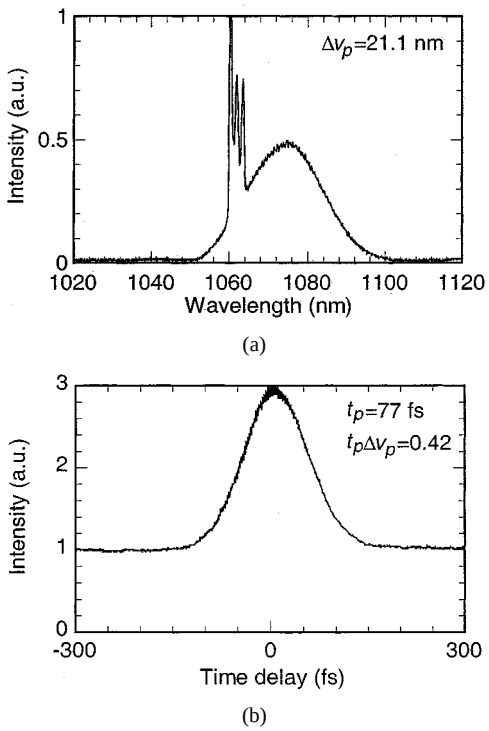

Fig. 13. (a) Spectrum and (b) autocorrelation trace of self-sustained pulses with $k''p_m = -1200$ fs^2.

autocorrelation trace with the AOM on has large fluctuations in the background. A probable reason is that the resonant dispersion causes a drift of the pulse from the transmission peak of the modulation function. The walk-off between the soliton-like pulse and transmission peak of the AM modulation might lead to a periodic perturbation of the soliton-like pulse. However, in self-sustained operation this walk-off of synchronization does not exist. To keep a soliton-like pulse stable, some amplitude modulation must be present [4], [15]. In the absence of the active amplitude modulation, we conclude that it is the Kerr-lens modelocking (KLM) effect that provides the passive amplitude modulation and keeps the soliton-like pulse stable. We identified the KLM to be linked to a hard-aperture effect through slightly cutting the intracavity laser beam either at the edge of the AOM or by a knife-edge inserted into the cavity [16]. The Kerr-lens effect was further confirmed by examining the spatial profile of the output beam in both the free-running and self-sustaining state [16]. We obtained self-sustained operation only when the negative GVD was larger than -900 fs^2. With a larger negative GVD, the self-sustained operation was easier to achieve, and the autocorrelation trace was smoother.

In this experiment, we kept the pulse bandwidth at about 4–5 nm without purposely flattening the gain profile. After optimization of the modelocking conditions, we were able to obtain a very broad pulse spectrum, and thus, sub-100-fs pulses [8], [16]. The optimization includes reshaping the gain profile by introducing more loss for the shorter wavelength components with partial beam cutting by the prism near the output mirror, increasing the intracavity energy (corresponding to an output power of $\sim$40 mW), and enhancing the KLM effect by inserting an intracavity knife-edge near the AOM. The shortest self-sustaining pulses are about 77 fs when $k''p_m \approx -1200$ fs^2. The pulse spectrum and pulse autocorrelation are shown in Fig. 13. The KLM effect in our experiment was still weak, though, and could not completely remove some low intensity noise background that coexisted with the mode-locked pulse and appeared as a narrow spike over the pulse spectrum [17]. By using two pieces of Nd : silicate glass plates to enhance the KLM, the noise background was able to be removed completely, and the spectrum became clean [16]. Most of the time the active modulation was required to start the self-sustained modelocking process. Occasionally, we observed, without the AM modulation, generation of self-sustaining femtosecond pulses by knocking the table or the end mirror. We have not obtained complete self-starting of modelocking without AM modulation or an external perturbation.

IV. Conclusion

We have comprehensively studied the modelocking performance of an actively mode-locked inhomogeneously broadened laser in different GVD regions through numerical simulation and experiment. In the positive GVD region, the dispersion and the SPM impede the generation of coherent and short pulses for a broad-band inhomogeneously broadened laser. In the negative GVD region, the generation of a single soliton-like pulse is limited within a certain range of negative GVD. In the small negative GVD region, the gain linewidth limits the spectral broadening, and thus the laser can only generate multiple soliton-like spikes. When the negative GVD becomes too large, the nonsoliton spectral components destabilize the soliton-pulse shaping process, and the laser generates again only incoherent pulses. With a weak SAM, self-sustained modelocking can be achieved, while self-starting of modelocking is not attainable. The experiment with an actively mode-locked Nd : silicate glass laser confirms the GVD dependence of actively mode-locked inhomogeneously broadened lasers.

REFERENCES

[1] D. J. Kuizenga and A. E. Siegman, "FM and AM mode-locking of the homogeneous laser—Part I: Theory," *IEEE J. Quantum Electron.*, vol. QE-6, pp. 694–708, 1970.

[2] J. T. Darrow and R. K. Jain, "Active mode locking of broad band continuous wave lasers," *IEEE J. Quantum Electron.*, vol. 27, pp. 1048–1060, Apr. 1991.

[3] H. A. Haus and Y. Silberberg, "Laser mode locking with addition of nonlinear index," *IEEE J. Quantum Electron.*, vol. QE-22, pp. 325–331, 1986.

[4] F. X. Kärtner, D. Kopf, and U. Keller, "Solitary-pulse stabilization and shortening in actively mode-locked lasers," *J. Opt. Soc. Amer. B*, vol. 12, pp. 486–496, 1995.

[5] J. Zhou, G. Taft, C.-P. Huang, M. M. Murnane, and H. C. Kapteyn, "Pulse evolution in a broad-bandwidth Ti : sapphire laser," *Opt. Lett.*, vol. 19, pp. 1149–1151, 1994.

[6] L. Yan, P.-T. Ho, C. H. Lee, and G. L. Burdge, "Generation of ultrashort pulses from a neodymium glass laser system," *IEEE J. Quantum Electron.*, vol. 25, pp. 2431–2440, Dec. 1989.

[7] L. Yan, "Pulse coherence of actively mode-locked inhomogeneously broadened lasers," *Opt. Commun.*, vol. 162, pp. 75–78, 1999.

[8] W. Lu, L. Yan, and C. R. Menyuk, "Self-sustaining sub-100 fs pulse generation from an actively mode-locked Nd : glass laser," *OSA Trends Opt. and Photon.*, vol. 50, pp. 582–584, 2001.

[9] L. Yan, "Continuous-wave lasing of hybrid lasers," *IEEE J. Quantum Electron.*, vol. 33, pp. 1075–1083, July 1997.

[10] G. P. Agrawal, *Nonlinear Fiber Optics*. San Diego, CA: Academic, 1995, ch. 3.

[11] T. Brabec, Ch. Spielmann, and F. Krausz, "Mode locking in solitary lasers," *Opt. Lett.*, vol. 16, pp. 1961–1993, 1991.

[12] D. W. Hall, R. A. Haas, W. F. Krupke, and M. J. Weber, "Spectral and polarization hole burning in neodymium glass lasers," *IEEE J. Quantum Electron.*, vol. 19, pp. 1704–1717, June 1993.

[13] D. W. Hall, M. J. Weber, and R. T. Brundage, "Fluorescence line narrowing in neodymium laser glasses," *J. Appl. Phys.*, vol. 55, pp. 2642–2647, 1984.

[14] D. W. Hall and M. J. Weber, "Modeling gain saturation in neodymium laser glasses," *IEEE J. Quantum Electron.*, vol. QE-20, pp. 831–834, 1984.

[15] H. A. Haus, J. G. Fujimoto, and E. P. Ippen, "Structures for additive pulse mode locking," *J. Opt. Soc. Amer. B*, vol. 8, pp. 2068–2076, 1991.

[16] W. Lu, L. Yan, and C. R. Menyuk, "Kerr-lens mode locking of Nd : glass laser," *Opt. Commun.*, vol. 200, pp. 159–163, 2001.

[17] D. E. Spence and W. Sibbett, "Femtosecond pulse generation by a dispersion-compensated, coupled-cavity, mode-locked Ti : sapphire laser," *J. Opt. Soc. Amer. B*, vol. 8, pp. 2053–2060, 1991.

Wei Lu was born in 1972. He received the B.S. and M.S. degrees from Zhejiang University, Hangzhou, China, in 1994 and 1997, respectively. He is currently working toward the Ph.D. degree in electrical engineering at the University of Maryland at Baltimore County, where his research is focused on ultrashort pulse generation from inhomogeneously broadened lasers.

Li Yan (S'89–M'89) received the B.S. degree from the University of Science and Technology of China in 1982 and the M.S. and Ph.D. degrees from the University of Maryland at College Park in 1986 and 1989, respectively.

After a Research Associate position at the University of Maryland, he joined the faculty of the Department of Electrical Engineering, the University of Maryland at Baltimore County in 1990, where he is currently an Associate Professor. His main research areas are ultrafast lasers, optical communications, and nonlinear optics.

Dr. Yan is a Member of the IEEE Lasers and Electro-Optics Society and the Optical Society of America.

Curtis R. Menyuk (SM'88–F'98) was born in 1954. He received the B.S. and M.S. degrees from the Massachusetts Institute of Technology, Cambridge, in 1976, and the Ph.D. from the University of California at Los Angeles in 1981.

He has been a Research Associate with the University of Maryland at College Park and with Science Applications International Corporation, McLean, VA. In 1986, he became an Associate Professor in the Department of Electrical Engineering, University of Maryland at Baltimore County (UMBC), and was the founding member of this department. In 1993, he was promoted to Professor. From 1996–2001, he was with the Department of Defense (DoD), Adelphi, MD, codirecting (part-time) the Optical Networking Program at the DoD Laboratory for Telectommunications Science during 1999–2001. In August 2001, he left the DoD and became Chief Scientist at PhotonEx Corporation, Maynard, MA. For the last 15 years, his primary area of research has been theoretical and computational studies of fiber-optic communications. He has authored or coauthored more than 150 archival journal publications, as well as numerous other publications and presentations, and has edited two books. The equations and algorithms that he and his research group at UMBC have developed to model optical fiber transmission systems are used extensively in the telecommunications industry. Additionally, he is a former UMBC Presidential Research Professor.

Dr. Menyuk is a member of the Society for Industrial and Applied Mathematics and the American Physical Society, and a Fellow of the Optical Society of America.